# Optimization of Operating Conditions for CO₂ Methanation Process Using Design of Experiments

Chae-Eun Yeo [1], Minhye Seo [1], Dongju Kim [1], Cheonwoo Jeong [2], Hye-Sun Shin [2] and Suhyun Kim [1,*]

1   Plant Engineering Center, Institute for Advanced Engineering, Yongin 17180, Korea; yce@iae.re.kr (C.-E.Y.); minhye_s@iae.re.kr (M.S.); kimdongju@iae.re.kr (D.K.)
2   Research Institute of Industrial Science and Technology (RIST), 187-12 Geumho-ro, Gwangyang-si 57801, Korea; cjeong@rist.re.kr (C.J.); hyesunshin@rist.re.kr (H.-S.S.)
*   Correspondence: shkim0605@iae.re.kr; Tel.: +82-31-330-7881

**Abstract:** In this study, the Taguchi experimental design method using an L16 orthogonal array was attempted in order to investigate the optimal operating conditions for the $CO_2$ methanation process in Ni-based catalysts. The relative influence of the main factors affecting $CO_2$ conversion and $CH_4$ yield was ranked as follows: reactor pressure > space velocity > reaction temperature. The optimal combination of operating conditions was a reactor temperature of 315 °C, a pressure of 19 bar, and a space velocity of 6000 $h^{-1}$. The effect of the $H_2/CO_2$ ratio on $CO_2$ conversion and $CH_4$ yield was further considered under these optimal operating conditions. Moreover, the catalyst was characterized in order to investigate the production of coke through Brunauer–Emmett–Teller analysis, thermogravimetric analysis, and scanning electron microscopy. The amount of coke produced after the reaction for approximately 24 h was ~2 wt.%. Therefore, the desired $CH_4$ yield and long-term operational stability were successfully obtained using the Taguchi design method and catalyst characterization.

**Keywords:** $CO_2$ methanation; power to gas; Taguchi method; design of experiments; coking

## 1. Introduction

Environmental issues such as air pollution and global warming have led to increasing efforts to reduce the use of fossil fuels worldwide and replace them with renewable energy sources, such as solar and wind energy. The main limitations to increasing the production of renewable electricity are intermittency and dispersion [1], which require efficient energy-storage technology. The imbalance between production and demand can create serious supply problems despite the availability of low-cost, renewable energy sources. In this context, power-to-gas (PtG) technology is an energy-storage technology that has been rapidly developed and is already being commercialized in Europe to improve energy storage. PtG technology converts surplus energy from renewable sources into combustible chemicals, which are easier to store and transport compared to electrical energy [2]. The PtG process consists of two steps: hydrogen ($H_2$) production through water electrolysis, and methane ($CH_4$) synthesis using CO or $CO_2$ [3]. These $H_2$ and $CH_4$ products produced using the PtG process have excellent storage capacity for extended periods [4]. In particular, the use of $CH_4$ is more desirable owing to its energy density, which is three times higher than that of $H_2$, and to the widespread facilities for its storage and transport [2,5,6]. Methane can be injected and stored into existing gas distribution grids or utilized in natural gas facilities [7].

The $CO_2$ methanation reaction, also known as the Sabatier process, is as follows:

$$CO_2 + 4H_2 \ = \ CH_4 + Alarc2H_2O \ \Delta H_R \ = \ -165.1 \ kJ/mol \tag{1}$$

This reaction is strongly exothermic and is controlled by chemical equilibrium [8]. Owing to kinetic limitations, the $CO_2$ methanation process is mainly performed using Ni-based catalysts at low temperatures of 250–400 °C.

Because of thermodynamic equilibrium, undesirable competing reactions such as CO methanation and the reverse water–gas shift reaction can occur at high temperature as follows:

$$CO + 3H_2 = CH_4 + H_2O \ \Delta H_R = -206.3 \ kJ/mol \tag{2}$$

$$CO_2 + H_2 = CO + H_2O \ \Delta H_R = 41.2 \ kJ/mol \tag{3}$$
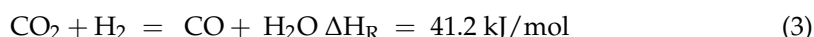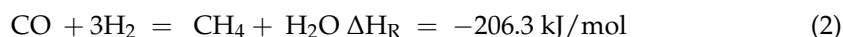
Therefore, one of the main issues in reactor scale-up is to remove heat generated by this exothermic reaction and maintain the process at a relatively low temperature, without generating hot spots or quenching the reaction [9]. Moreover, the operation must be performed at an appropriate temperature range to prevent unwanted competing reactions, and an adequate pressure is important for process optimization. A pressure increase up to a certain point can improve the reaction efficiency in a general temperature range [10,11]. However, a technical–economic compromise is necessary because the compressor power consumed to increase the water electrolysis hydrogen supply pressure can be greater than the increase in methane and steam production.

Several operating parameters are closely related to the performance of methane production. Extensive studies of $CO_2$ methanation have been conducted to determine the effect of operating variables; relevant details are summarized in Table 1.

**Table 1.** Summary of experimental studies on $CO_2$ methanation.

| Operating Parameters | Reactor Type | Catalyst | Reference |
|---|---|---|---|
| Temperature: 250–550 °C<br>Reaction cycle, Metal loading amount<br>($H_2/CO_2 = 5$; SV = 5835 $h^{-1}$) | Packed-bed reactor | $Ni/Al_2O_3$,<br>$Ru/Al_2O_3$,<br>$Ru$-$Ni/Al_2O_3$ | [7] |
| $H_2/CO_2$: 1–5<br>Pressure: 1–100 atm<br>Temperature: 200–600 °C<br>$H_2/CO_2/H_2O$: 4/1/(0–0.5)<br>$H_2/CO_2/O_2$: 4/1/(0–0.5) | Fixed-bed reactor | Ni-based catalyst | [10] |
| Gas flow rate: 9.9–23 $Nm^3/h$<br>$H_2/CO_2$: 3.72–4.2<br>Pressure: 1.5–3.0 bar<br>Temperature: 280–350 °C | Microchannel reactor | Ni-based catalyst | [12] |
| Pressure: 1–10 bar<br>Temperature: 250–400 °C | Triple fixed-bed reactor | $Ni/Al_2O_3$ catalyst | [13] |
| GHSV: 5760–23,000 L $kg^{-1}$ $h^{-1}$<br>$H_2/CO_2$: 1.0–4.2<br>Temperature: 100–600 °C | Fixed-bed reactor | Ni-based catalyst<br>(Ni-MCM-41) | [14] |
| WHSV: 6000–11,500 $Ncm^3/g{\cdot}h$<br>$H_2/CO_2$: 4.3–4.5<br>Pressure: 1–5 bar | Multi-tubular fixed-bed reactor | 0.5 wt.% Ru on $Al_2O_3$ | [15] |

Factors that influence $CO_2$ methanation performance include reactor temperature, pressure, space velocity, and $H_2/CO_2$ ratio. A high $CO_2$ conversion and $CH_4$ yield can be used as performance indicators for maximum methane gas production. Several experiments for evaluating $CO_2$ methanation have been conducted to investigate the effect of one parameter at a time. However, this approach is time-consuming and labor-intensive [16]. Optimization tools can be used to identify the best output for optimal methane gas production based on input values in less time and with lower costs. The Taguchi optimization method is an efficient approach for optimizing performance with minimal experimentation.

Therefore, the Taguchi design of experiment approach can be used to optimize methane production with minimal time and low cost.

The main objective of this study was to optimize $CO_2$ methanation using the Taguchi method to determine the effects of reactor temperature, pressure, space velocity, and $H_2/CO_2$ ratio. Because of economic limitations such as operating costs and difficulty in obtaining a sufficient amount of catalyst, pre-evaluation of catalysts or feedstocks and the selection of operating conditions to optimize product yield are typically performed in laboratory and pilot-scale reactors. Therefore, optimizing reaction conversion and product yields is a starting point for scale-up to pilot and commercial $CO_2$ methanation reactors. The most influential parameters and optimal operating conditions for methane production were investigated using the Taguchi experimental design with an L16 orthogonal array. In addition, considering the formation of coke on the catalyst surface, which occurs during methanation, we verified the high performance and durability of the catalyst. During the reactor scale-up process, we investigated possible variations in process factors, such as the $H_2/CO_2$ ratio, by minimizing trial and error in the operation and coordination of economic aspects when product productivity and quality above a certain level were secured. Finally, the stability of catalyst activity was evaluated through coking analysis using $H_2/CO_2$ under the optimal conditions selected by the Taguchi method.

## 2. Materials and Methods

### 2.1. Catalyst Preparation

The catalyst used in this experiment was 40Ni5Mg-Al-Zeolite synthesized by the co-precipitation method, which contains 72 wt% NiO, 16 wt% $Al_2O_3$, and 12 wt% $SiO_2$. Nickel nitrate ($Ni(NO_3)_2.6H_2O$), Magnesium nitrate ($Mg(NO_3)_2.6H_2O$), and Aluminum nitrate ($Al(NO_3)_3.9H_2O$) were dissolved in distilled water. The solution temperature was raised to 50 °C while stirring the solution using an overhead stirrer. Then, aqueous ammonia was added dropwise to the solution to precipitate solid particles until pH 7 was reached. After the reaction was carried out for 3 h, the filtered solid powder was dried at 110 °C overnight. The solid material obtained was calcined at 500 °C for 5 h. The prepared catalyst was mixed with a binder (graphite 5%) and zeolite (Chabazite, Si/Al = 16, 10%) and then calcined at 600 °C for 5 h. The catalyst was used in the form of a pellet (diameter = 5 mm, height = 7 mm) with a specific surface area of 161.1 $m^2/g$ and a micropore volume of 0.027 $cm^3/g$.

### 2.2. Catalyst Activity Test

2.2.1. Experimental Apparatus

$CO_2$ methanation experiments under various operating conditions were performed in a fixed-bed reactor (ID = 10 mm, height = 60 mm). The mesh was installed to support the catalyst bed inside the reactor, and 1 g of the catalyst was filled in the catalyst bed.

Preheated feed gases ($N_2$ as an inert gas, $H_2$, and $CO_2$) were injected into the reactor and controlled by a mass flow meter at a specific $H_2/CO_2$ ratio. In addition, $N_2$ was used as the reference flow rate to evaluate the flow of product gas exiting the reactor. Thermocouples were inserted at the top and bottom of the reactor to measure the temperature of the catalyst bed and the temperature inside the reactor. The reactor temperature was controlled by an external heating jacket surrounding the reactor. The pressure was controlled by a back-pressure regulator located at the rear end of the condenser (Figure 1).
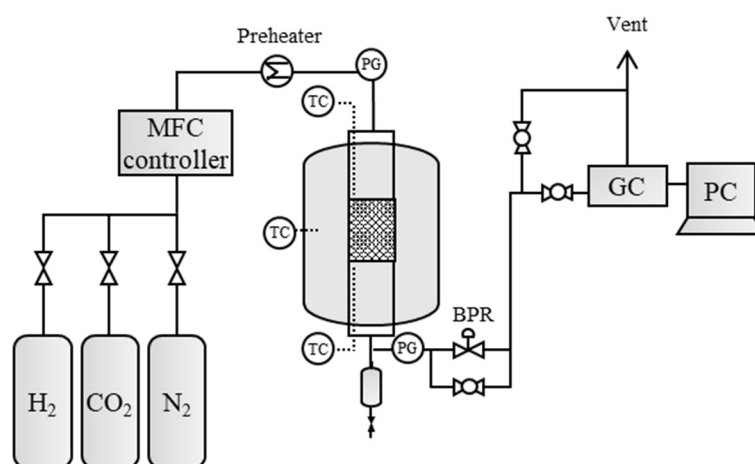
**Figure 1.** Schematic diagram of the experimental apparatus.

### 2.2.2. Data Analysis

A 2Ch-MicroGC (3000 MicroGC Gas Analyzer, Inficon Co., Bad Ragaz, Switzerland) was used to analyze the components of the gas product. The gas from the reactor was dewatered from the condenser and flowed through a filter into a gas chromatograph (GC). The concentration of the gas was then measured in real time in the GC. To ensure the reliability of the reaction, the stream measurement time for each test was at least 2 h. Two columns were used to analyze the cooled reaction gas: Mol-Sieve5A (10 m × 0.32 mm × 30 μm, Inficon) and Plot U (8 m × 0.32 mm × 30 μm, Inficon). To reduce the delay in the analysis of the reaction gas, a PLOT U column was additionally placed on the Mol-Sieve5A column and injected by using a back-flush pretreatment. A micro-thermal conductivity detector was used, and the temperature of the column oven was maintained at 70 °C. Argon was used as the carrier gas for the Mol-Sieve5A column, and helium was used for the PLOT U column. As the reaction gas passed through the column for 240 s, chromatograms of hydrogen, nitrogen, oxygen, carbon monoxide, and methane were obtained from the Mol-Sieve5A column. In addition, the chromatogram of $CO_2$ was obtained from the PLOT U column, and quantitative analysis at the ppm level was performed by calibrating the curve using a standard gas.

The reaction performance was evaluated using Equations (4)–(6).

$$X_{CO2}(\%) \ = \ (F_{CO2,in} - F_{CO2,out})/F_{CO2,in} \times 100 \tag{4}$$

$$S_{CH4}(\%) \ = \ F_{CH4}/(F_{CH4} + F_{Co2,out}) \times 100 \tag{5}$$

$$Y_{CH4}(\%) \ = \ X_{CO2} \times S_{CH4}/100 \tag{6}$$

where $Xi$ is the conversion of $i$ species, $Fi$ is the molar flow rate, $Si$ is the selectivity, and $Yi$ is the yield.

### 2.3. Taguchi Experimental Design Method

The Taguchi design method was performed using Minitab 20 software to determine the optimal operating conditions for $CO_2$ methanation. The optimal values of all parameter combinations may not be within the same ranges used in the experimental design. Nevertheless, the Taguchi design method was used to increase the efficiency of the experiments by minimizing time loss [17,18].

Based on previous studies, the temperature, pressure, and space velocity of the reactor were selected as the main factors affecting the performance of $CO_2$ methanation. Table 2 shows the factors and levels used in this study.

**Table 2.** Experimental parameters and their levels for the Taguchi design.

| | Factor | Unit | Level 1 | Level 2 | Level 3 | Level 4 |
|---|---|---|---|---|---|---|
| A | Temperature | °C | 280 | 315 | 350 | 385 |
| B | Pressure | bar | 1 | 7 | 13 | 19 |
| C | Space velocity | h$^{-1}$ | 6000 | 13,500 | 21,000 | 28,500 |

An orthogonal array with different combinations of input parameters was designed using the Taguchi method. The Taguchi L16 array, including three factors and four levels for analysis, is shown in Table 3.

**Table 3.** L16 orthogonal array used in this study.

| No. | Factor A | Factor B | Factor C |
|---|---|---|---|
| | Temperature (°C) | Pressure (Bar) | Space Velocity (H$^{-1}$) |
| 1 | 280 | 1 | 6000 |
| 2 | 280 | 7 | 13,500 |
| 3 | 280 | 13 | 21,000 |
| 4 | 280 | 19 | 28,500 |
| 5 | 315 | 1 | 13,500 |
| 6 | 315 | 7 | 6000 |
| 7 | 315 | 13 | 28,500 |
| 8 | 315 | 19 | 21,000 |
| 9 | 350 | 1 | 21,000 |
| 10 | 350 | 7 | 28,500 |
| 11 | 350 | 13 | 6000 |
| 12 | 350 | 19 | 13,500 |
| 13 | 385 | 1 | 28,500 |
| 14 | 385 | 7 | 21,000 |
| 15 | 385 | 13 | 13,500 |
| 16 | 385 | 19 | 6000 |

In the Taguchi method, controllable factors are termed parameters, whereas uncontrollable factors are referred to as noise (N). The method used to calculate the signal-to-noise (S/N) ratio can be classified into three types: larger is better, nominal is best, and smaller is better. In this study, the larger is better rule was adopted with the goal of maximizing the $CO_2$ conversion rate [19]. The S/N ratio can clarify the quantitative characteristics of the process parameters and products. It was calculated as follows:

$$S/N \ ratio \ = \ -10 \log 1/y^2/n \tag{7}$$

where $y$ is the $CO_2$ conversion or $CH_4$ yield, and $n$ is the number of factor level combination reactions.

### 2.4. Catalyst Characterization

2.4.1. Qualitative Analysis of Catalyst Characterization

The specific surface area of the catalyst was measured based on the $N_2$ adsorption/desorption isotherm, which was determined using a Brunauer–Emmett–Teller (BET) analyzer (Tristar II 3020, Micromeritics, Norcross, GA, USA). During pre-treatment, the sample was degassed under vacuum at 150 °C for 1 h. The BET method was then used to calculate the specific surface area.

A field scanning electron microscope (Mira3, Tescan, Kohoutovice, Czech Republic) was used to analyze the surface structure of the catalyst. After drying the catalyst sample at 120 °C for approximately 1 h, the catalyst was coated with a metal, and nitrogen was added under vacuum. The surface structure of the catalyst before and after the reaction was determined from scanning electron microscopy (SEM) images.

### 2.4.2. Quantitative Analysis of Coke Production

After 16 sets of experiments consisting of a Taguchi orthogonal array, additional tasks were performed for each $H_2/CO_2$ ratio under the determined optimal conditions. A thermogravimetric analyzer (DTG-60, Shimadzu, Kyoto, Japan) was used to investigate the coke produced in the catalyst after the $CO_2$ methanation. The temperature was raised to 800 °C at a heating rate of 10 °C/min under an air atmosphere. This temperature was maintained for 5 min, while the sample mass was measured. The equation used to calculate the mass of coke produced was as follows:

$$W_c(\text{wt\%}) = \frac{M_{t,b} - M_{t,a}}{M_{t,a}} \times 100 \tag{8}$$

where $W_c$ is the coke weight percent (wt.%), and $M_{t,b}$ and $M_{t,a}$ are the sample mass before and after thermogravimetric analysis, respectively.

## 3. Results and Discussion

### 3.1. Taguchi Approach

Figure 2 shows the average S/N ratio plot for each factor based on the experimental results of the Taguchi L16 combination. The profile of each factor (Figure 2) indicates that the output factors ($CO_2$ conversion rate and $CH_4$ yield) did not increase or decrease according to the level change in each factor. For factor A (reactor temperature), the S/N ratio formed an inflection point at 315 °C. Tamimi et al. [20] reported that an increase in the reaction temperature up to 350 °C leads to higher $CO_2$ conversion, but a further temperature increase can decrease the conversion because of the thermodynamic limit. Although the degrees of influence of the pressure and space velocity on the conversion rate were different, the trends were similar to those in the results of several previous studies [14,20–23].
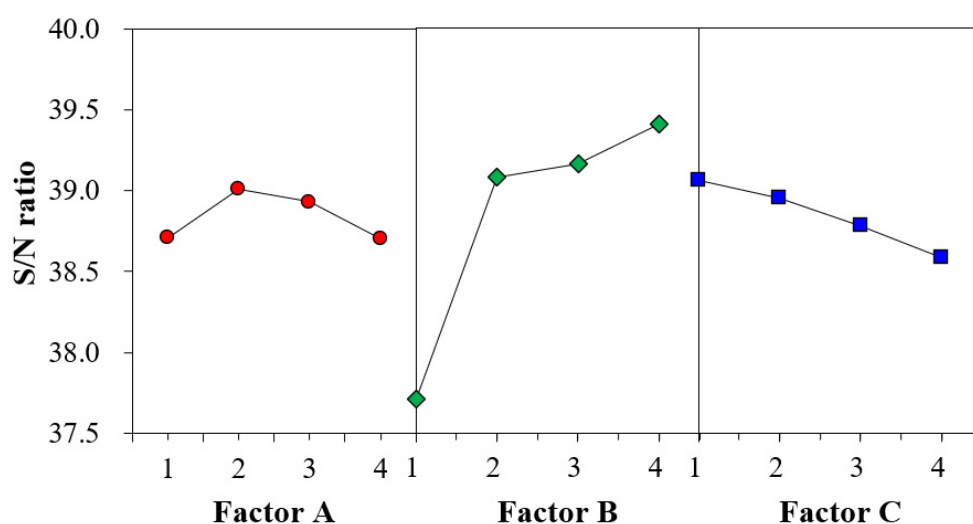


**Figure 2.** Primary effects of S/N ratio on $CO_2$ conversion and $CH_4$ yield.

A larger average S/N ratio leads to higher $CO_2$ conversion and $CH_4$ yield. The effect of each factor was calculated by subtracting the minimum S/N ratio from the factor's maximum S/N ratio [24,25]. The magnitude of change in the average S/N ratio indicates the magnitude of influence of each factor on $CO_2$ conversion and $CH_4$ yield. The effects of temperature, pressure, and space velocity are shown in Figure 3a.
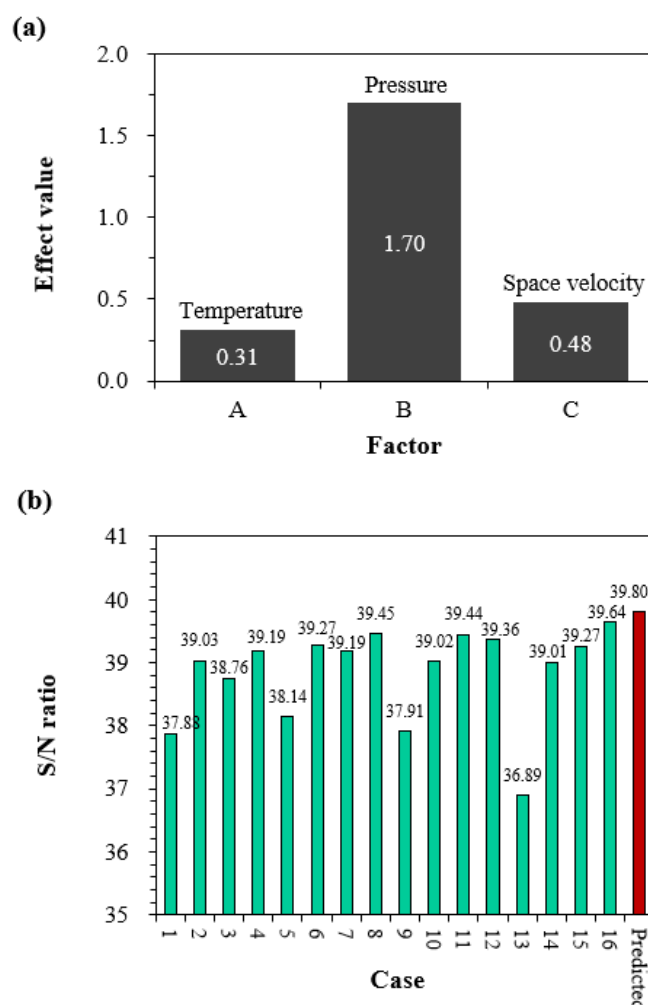
**Figure 3.** Profiles of (**a**) effect value in terms of $CO_2$ conversion and $CH_4$ yield, and (**b**) mean S/N ratios for 16 cases of orthogonal array and optimal combinations.

A higher effect value suggests a greater effect on the yield and conversion rate of $CO_2$ methanation. Figure 3 shows that the relative influence of the factors was ranked as reactor pressure (Factor B) > space velocity (factor C) > temperature (factor A), and the influence of pressure (factor B) on $CO_2$ conversion and $CH_4$ yield was clearly more pronounced than that of the other two factors. The optimal conditions for $CO_2$ methanation were obtained by selecting and combining the levels at the highest S/N ratio for each factor. As shown in Figures 2 and 3a, the combination of optimal conditions for each factor that led to the highest S/N ratio corresponded to the second level in factor A, the fourth level in factor B, and the first level in factor C. This result indicates that a reactor temperature of 315 °C, a pressure of 19 bar, and a space velocity of 6000 $h^{-1}$ formed the optimal combination of operating conditions. Figure 3b shows the S/N ratio profile of the experimental results obtained using a Taguchi L16 array design combination, including the S/N ratio for the optimal combination.

Catalyst reactions are fundamentally complex phenomena, and their productivity is affected by several interactions. Therefore, the optimization results can be influenced by the effects of interactions. Potential interactions between different control factors can be interpreted as the magnitude of the difference between the predicted performance and the validation experiment [24]. Accordingly, a verification experiment was performed because the obtained combination of the three optimal conditions was not included in the previously performed Taguchi L16 array.

Table 4 shows the verification results of the experiments analyzing the parameter combination A2B4C1. The experimental results were compared to the predicted values. The relative difference (in percent) in the S/N ratio was 0.87, and the predicted value for each combination was close to the experimentally measured value. The differences between the predicted and the experimental responses were attributed to the interaction between parameters. The $H_2/CO_2$ ratio is among the main factors determining the $CO_2$ methanation performance, along with temperature, pressure, and space velocity. Therefore, the effect of the $H_2/CO_2$ ratio on the methanation reaction was investigated under the optimal combination of operating conditions obtained by the Taguchi L16 orthogonal array experiment. A $H_2/CO_2$ range of 3.6–4.0 was selected to ensure sufficient methane yield in commercial plants and maintain long-term performance.

**Table 4.** Validation results from experiments for optimal parameter combination.

| Parameter Combination | Predicted | Experimental Confirmation | Relative Difference (%) |
|---|---|---|---|
| | S/N Ratio | S/N Ratio | |
| A2B4C1 | 39.80 | 39.45 | 0.87 |

### 3.2. Catalytic Performance

Figure 4 shows the effect of the $H_2/CO_2$ ratio on the $CO_2$ conversion and $CH_4$ yield at 315 °C, a pressure of 19 bar, and a space velocity of 6000 $h^{-1}$, which were the operating conditions of the optimal combination. The catalytic performance was found to be similar to the thermodynamic equilibrium value [6]. The $CO_2$ conversion and $CH_4$ yield increased as the $H_2/CO_2$ ratio increased from 3.6 to 4.0. The quality and production capacity of methane can be affected by potential and complex interactions between several factors. For instance, increasing the $H_2/CO_2$ molar ratio in the reactant increases the $CO_2$ conversion rate by increasing the amount of $H_2$ that can react with $CO_2$ [20,26]. However, an excessive amount of $H_2$ can increase the amounts of $CH_4$ produced and the amounts of unreacted $H_2$; thus, the economic aspects of this reaction should be carefully evaluated.
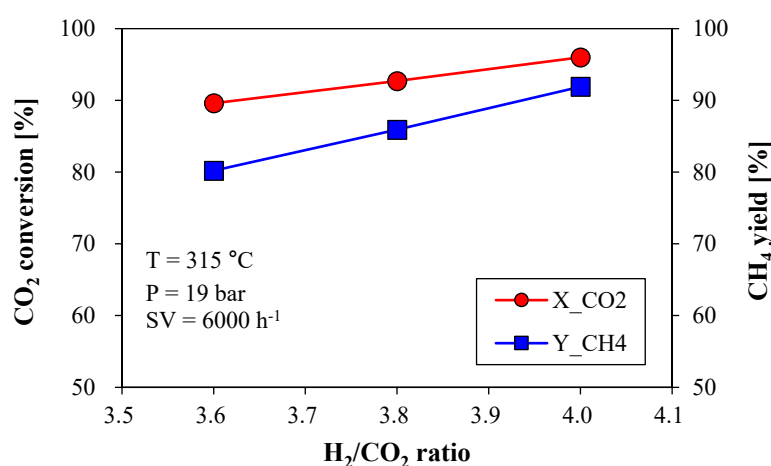


**Figure 4.** Effect of $H_2/CO_2$ on $CO_2$ conversion and $CH_4$ yield at 315 °C, 19 bar, and 6000 $h^{-1}$.

Deactivation of the catalyst by coke is very important for catalysts used in the industrial field. Accumulation of coke in the catalyst bed may prevent the injected gas from passing through the catalyst bed and thereby cause backflow. Therefore, we investigated the performance of the overall process by considering the potential for catalyst coking obtained in the experiments using different $H_2/CO_2$ ratios.

Figure 5 shows the amount of coke produced after the reaction at $H_2/CO_2$ = 3.6, 3.8, and 4.0. The amount of coke produced was compared based on the wt.%. Coke production

increased by approximately 1.2–1.8 times as the $H_2/CO_2$ ratio increased from 3.6 to 4.0. Ocampo et al. [21] reported that a lack of hydrogen can promote catalyst deactivation. However, under all three conditions, the amount of coke generated (approximately 2 wt.%) was considered insignificant compared to the total amount of catalyst. Therefore, the operating conditions can be adjusted while considering the economic balance if a production capacity above a certain level is guaranteed.
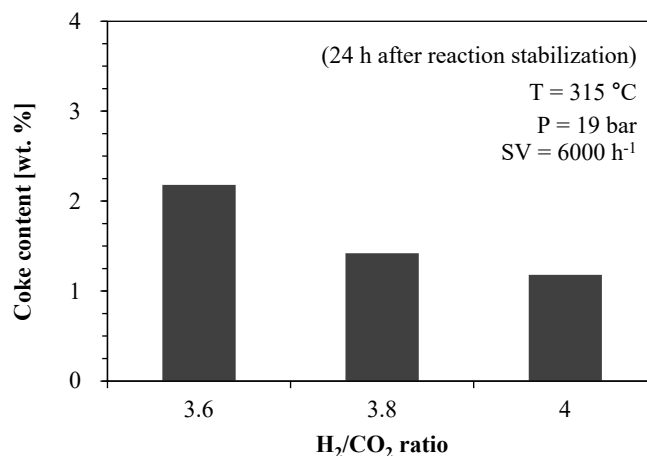


**Figure 5.** Coke produced during $CO_2$ methanation at different $H_2/CO_2$ molar ratios.

Table 5 shows the specific surface area and pore volume of the catalyst particles measured according to the BET method by $N_2$ gas adsorption. The BET surface area was approximately 80–82% of that of the fresh catalyst. The volume of 1.7–300 nm pores slightly decreased compared to the fresh catalyst as the $CO_2$ methanation proceeded, but the effect of the $H_2/CO_2$ ratio was small or insignificant. Previous studies showed that alumina sinter easily under hydrothermal conditions, contributing to the reduction in the BET surface area [27]. The formation of deposits and pore clogging on the catalyst surface may decrease the specific surface area, which can decrease the $CO_2$ conversion rate. The degree of influence of the $H_2/CO_2$ ratio on the BET surface area and pore volume was distributed at almost the same level.

**Table 5.** BET analysis of catalysts after $CO_2$ methanation for 24 h.

| $H_2/CO_2$ | Bet Surface Area ($m^2/g$) | 1.7 nm–300 nm Pore Volume ($cm^3/g$) | Total Pore Volume ($cm^3/g$) |
|---|---|---|---|
| 3.6 | 129.2 | 0.24 | 0.298 |
| 3.8 | 130.1 | 0.24 | 0.300 |
| 4.0 | 132.8 | 0.25 | 0.298 |
| Fresh catalyst | 161.1 | 0.26 | 0.301 |

The presence of carbon deposits on the catalyst surface was observed by using SEM. Figure 6 shows the SEM images after $CO_2$ methanation of the surface morphology and after carbon deposition changes in the catalyst for each $H_2/CO_2$ ratio. Figure 6a–c shows that the pore structure was lost because of gradual thermal fatigue as compared to the fresh catalyst shown in Figure 6d. The carbon deposition on the catalyst surface appeared to slightly intensify as the $H_2/CO_2$ ratio decreased, but the difference was negligible.
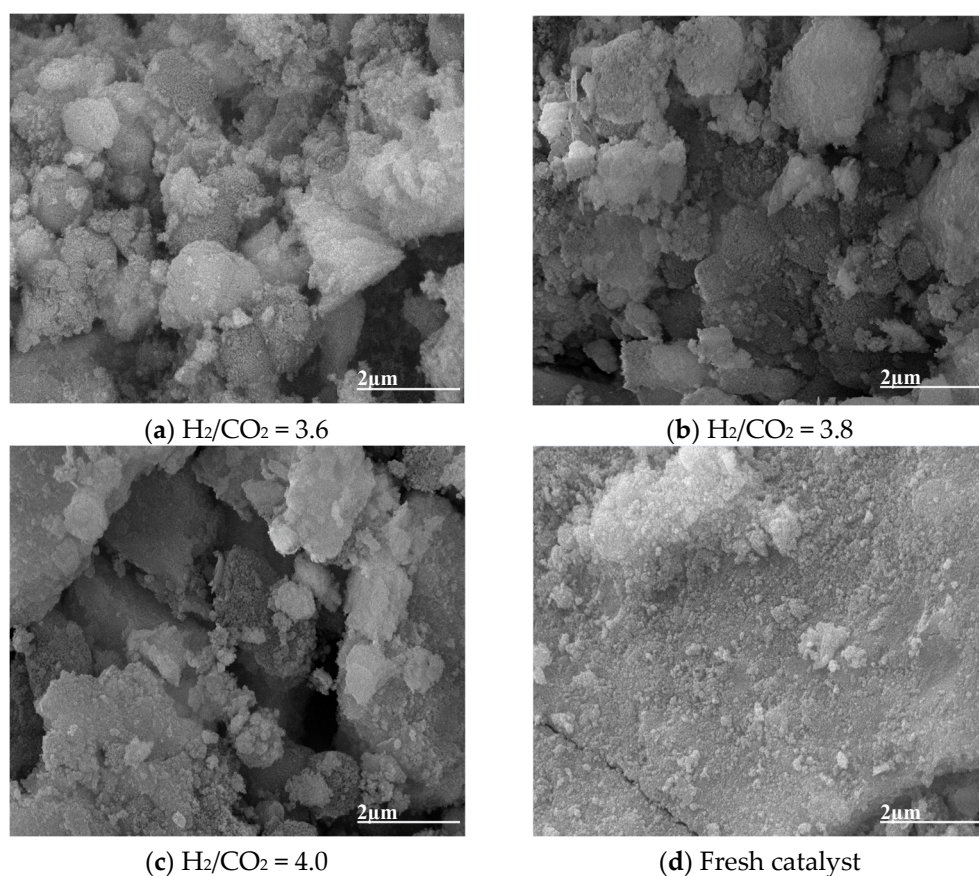
(**a**) $H_2/CO_2$ = 3.6      (**b**) $H_2/CO_2$ = 3.8





(**c**) $H_2/CO_2$ = 4.0      (**d**) Fresh catalyst

**Figure 6.** SEM images of catalysts after $CO_2$ methanation at $H_2/CO_2$ molar ratios of (**a**) 3.6, (**b**) 3.8, and (**c**) 4.0, and for (**d**) fresh catalyst.

The effects of the three $H_2/CO_2$ ratios ($H_2/CO_2$ = 3.6, 3.8, and 4.0) on $CO_2$ conversion and $CH_4$ yield were similar and led to nearly identical effects on carbon deposition. In other words, $H_2/CO_2$ molar ratios of 3.6–4.0 did not substantially affect the $CO_2$ methanation performance. Therefore, the results indicate that stable operation is possible under the optimal combination for $CO_2$ methanation obtained using the Taguchi design method within the $H_2/CO_2$ range of 3.6–4.0.

## 4. Conclusions

We optimized the operating conditions of $CO_2$ methanation using the Taguchi design method. The $CH_4$ yield was maximized by selecting the output factor ($CO_2$ conversion) and efficient parameters. Reaction temperature, reactor pressure, and space velocity at three factors and four levels were investigated as influencing factors. The relative influence of these factors on $CO_2$ methanation experiments using a Taguchi L16 array were in the following order: reactor pressure (factor B) > space velocity (factor C) > reaction temperature (factor A). The optimal combination of operating conditions for $CO_2$ methanation was a reactor temperature of 315 °C, a pressure of 19 bar, and a space velocity of 6000 $h^{-1}$. The optimal combination of parameters that was obtained was verified through experiments, and the relative difference (in percent) between the predicted and the experimental S/N ratio was 0.87. We also investigated whether stable catalyst performance could be achieved under the selected operating conditions, as well as the degree to which the $H_2/CO_2$ ratio affects the $CO_2$ conversion rate and $CH_4$ yield. Based on a stoichiometric ratio of $H_2/CO_2$ = 4, the $CO_2$ conversion and $CH_4$ yield increased as the $H_2/CO_2$ ratio increased from 3.6 to 3.8. The amount of coke generated after the reaction was inversely proportional to the $H_2/CO_2$ ratio, but the amount of coke generated for all $H_2/CO_2$ ratios (3.6, 3.8, and 4.0) accounted for only approximately 2 wt.% of the

total sample mass. The results obtained using the Taguchi design method and catalyst characterization demonstrate that sufficient methane yield and long-term operational stability can be obtained at 315 °C, 9 bar, and 6000 h$^{-1}$ in the range of $H_2/CO_2$ = 3.6–4.0.

**Author Contributions:** Conceptualization, C.-E.Y.; investigation, C.-E.Y., C.J. and H.-S.S.; writing—original draft preparation, C.-E.Y., D.K.; writing—review and editing, C.-E.Y., M.S. and D.K.; visualization, C.-E.Y.; supervision, M.S. and S.K. All authors have read and agreed to the published version of the manuscript.

**Conflicts of Interest:** The authors declare no conflict of interest.

## References

1. Meylan, F.D.; Moreau, V.; Erkman, S. Material constraints related to storage of future European renewable electricity surpluses with $CO_2$ methanation. *Energy Policy* **2016**, *94*, 366–376. [CrossRef]
2. Momeni, M.; Soltani, M.; Hosseinpour, M.; Nathwani, J. A comprehensive analysis of a power-to-gas energy storage unit utilizing captured carbon dioxide as a raw material in a large-scale power plant. *Energy Convers. Manag.* **2021**, *227*, 113613. [CrossRef]
3. Blanco, H.; Faaij, A. A review at the role of storage in energy systems with a focus on Power to Gas and long-term storage. *Renew. Sustain. Energy Rev.* **2018**, *81*, 1049–1086. [CrossRef]
4. Götz, M.; Lefebvre, J.; Mörs, F.; Koch, A.M.; Graf, F.; Bajohr, S.; Kolb, T. Renewable Power-to-Gas: A technological and economic review. *Renew. Energy.* **2016**, *85*, 1371–1390. [CrossRef]
5. Dannesboe, C.; Hansen, J.B.; Johannsen, I. Catalytic methanation of $CO_2$ in biogas: Experimental results from a reactor at full scale. *React. Chem. Eng.* **2020**, *5*, 183–189. [CrossRef]
6. Schaaf, T.; Grünig, J.; Schuster, M.R.; Rothenfluh, T.; Orth, A. Methanation of $CO_2$-storage of renewable energy in a gas distribution system. *Energy Sustain. Soc.* **2014**, *4*, 1–14. [CrossRef]
7. Chein, R.Y.; Wang, C.C. Experimental Study on $CO_2$ Methanation over Ni/Al$_2$O$_3$, Ru/Al$_2$O$_3$, and Ru-Ni/Al$_2$O$_3$ Catalysts. *Catalysts* **2020**, *10*, 1112. [CrossRef]
8. Gruber, M.; Weinbrecht, P.; Biffar, L.; Harth, S.; Trimis, D.; Brabandt, J.; Blumentritt, R. Power-to-Gas through thermal integration of high-temperature steam electrolysis and carbon dioxide methanation-Experimental results. *Fuel Process. Technol.* **2018**, *181*, 61–74. [CrossRef]
9. Brooks, K.P.; Hu, J.; Zhu, H.; Kee, R.J. Methanation of carbon dioxide by hydrogen reduction using the Sabatier process in microchannel reactors. *Chem. Eng. Sci.* **2007**, *62*, 1161–1170. [CrossRef]
10. Gao, J.; Wang, Y.; Ping, Y.; Hu, D.; Xu, G.; Gu, F.; Su, F. A thermodynamic analysis of methanation reactions of carbon oxides for the production of synthetic natural gas. *RSC Adv.* **2012**, *2*, 2358–2368. [CrossRef]
11. Stangeland, K.; Kalai, D.; Li, H.; Yu, Z. $CO_2$ methanation: The effect of catalysts and reaction conditions. *Energy Procedia* **2017**, *105*, 2022–2027. [CrossRef]
12. Chwoła, T.; Spietz, T.; Więcław-Solny, L.; Tatarczuk, A.; Krótki, A.; Dobras, S.; Zdeb, J. Pilot plant initial results for the methanation process using $CO_2$ from amine scrubbing at the Łaziska power plant in Poland. *Fuel* **2020**, *263*, 116804. [CrossRef]
13. Türks, D.; Mena, H.; Armbruster, U.; Martin, A. Methanation of $CO_2$ on Ni/Al$_2$O$_3$ in a structured fixed-bed reactor—A scale-up study. *Catalysts* **2017**, *7*, 152. [CrossRef]
14. Du, G.; Lim, S.; Yang, Y.; Wang, C.; Pfefferle, L.; Haller, G.L. Methanation of carbon dioxide on Ni-incorporated MCM-41 catalysts: The influence of catalyst pretreatment and study of steady-state reaction. *J. Catal.* **2007**, *249*, 370–379. [CrossRef]
15. Bassano, C.; Deiana, P.; Lietti, L.; Visconti, C.G. P2G movable modular plant operation on synthetic methane production from $CO_2$ and hydrogen from renewables sources. *Fuel* **2019**, *253*, 1071–1079. [CrossRef]
16. Pant, A.; Rai, J.P.N. Bioremediation of chlorpyrifos contaminated soil by two phase bioslurry reactor: Processes evaluation and optimization by Taguchi's design of experimental (DOE) methodology. *Ecotoxicol. Environ. Saf.* **2018**, *150*, 305–311. [CrossRef]
17. Kang, K.; Azargohar, R.; Dalai, A.K.; Wang, H. Hydrogen production from lignin, cellulose and waste biomass via supercritical water gasification: Catalyst activity and process optimization study. *Energy Convers. Manag.* **2016**, *117*, 528–537. [CrossRef]
18. Özdemir, C.; Akın, A.N.; Yıldırım, R. Low temperature CO oxidation in hydrogen rich streams on Pt-SnO$_2$/Al$_2$O$_3$ catalyst using Taguchi method. *Appl. Catal. A Gen.* **2004**, *258*, 145–152. [CrossRef]
19. Chen, W.H.; Chiu, G.L.; Ong, H.C.; Lam, S.S.; Lim, S.; Ok, Y.S.; Kwon, E.E. Optimization and analysis of syngas production from methane and $CO_2$ via Taguchi approach, response surface methodology (RSM) and analysis of variance (ANOVA). *Fuel* **2021**, *296*, 120642. [CrossRef]
20. Tamimi, K.; Alavi, S.M.; Rezaei, M.; Akbari, E. Preparation of the Mn-Promoted NiO–Al$_2$O$_3$ nanocatalysts for low temperature $CO_2$ methanation. *J. Energy Inst.* **2021**, *99*, 48–58. [CrossRef]

21. Ocampo, F.; Louis, B.; Kiennemann, A.; Roger, A.C. $CO_2$ methanation over Ni-Ceria-Zirconia catalysts: Effect of preparation and operating conditions. *IOP Conf. Ser. Mater. Sci. Eng.* **2011**, *19*, 012007. [CrossRef]

22. Han, D.; Kim, Y.; Byun, H.; Cho, W.; Baek, Y. $CO_2$ methanation of biogas over 20 wt% Ni-Mg-Al catalyst: On the effect of $N_2$, $CH_4$, and $O_2$ on $CO_2$ conversion rate. *Catalysts* **2020**, *10*, 1201. [CrossRef]

23. Guilera, J.; Boeltken, T.; Timm, F.; Mallol, I.; Alarcón, A.; Andreu, T. Pushing the limits of SNG process intensification: High GHSV operation at pilot scale. *ACS Sustain. Chem. Eng.* **2020**, *8*, 8409–8418. [CrossRef]

24. Shah, M.; Mondal, P. Optimization of $CO_2$ reforming of methane process for the syngas production over Ni–Ce/$TiO_2$–$ZrO_2$ catalyst using the Taguchi method. *Int. J. Hydrog.* **2021**, *46*, 22799–22812. [CrossRef]

25. Chen, C.J.; Hung, C.I. Optimization of co-gasification process in an entrained-flow gasifier using the Taguchi method. *J. Therm. Sci. Technol.* **2013**, *8*, 190–208. [CrossRef]

26. Aziz, M.A.A.; Jalil, A.A.; Triwahyono, S.; Mukti, R.R.; Taufiq-Yap, Y.H.; Sazegar, M.R. Highly active Ni-promoted mesostructured silica nanoparticles for $CO_2$ methanation. *Appl. Catal. B Environ.* **2014**, *147*, 359–368. [CrossRef]

27. Johnson, M.F. Surface area stability of aluminas. *J. Catal.* **1990**, *123*, 245–259. [CrossRef]